KU LEUVEN

WP EN2016-10

Comparison of series/parallel configuration for a low-T geothermal CHP plant, coupled to thermal networks

Sarah Van Erdeweghe, Johan Van Bael, Ben Laenen, William D'haeseleer

TME WORKING PAPER - Energy and Environment
Last update: April 2017

KULeuven Energy Institute
TME Branch

Comparison of series/parallel configuration for a low-T geothermal CHP plant, coupled to thermal networks

Sarah Van Erdeweghe[a,c], Johan Van Bael[b,c], Ben Laenen[b], William D'haeseleer[a,c,*]

[a] *KU Leuven (University of Leuven), Applied Mechanics and Energy Conversion Section, Celestijnenlaan 300 - box 2421, B-3001 Leuven, Belgium*

[b] *Flemish Institute of Technological Research (VITO), Boeretang 200, B-2400 Mol, Belgium*

[c] *EnergyVille, Thor Park, Poort Genk 8310, B-3600 Genk, Belgium*

Abstract

In this paper, the performance of a low-temperature ($130°C$) geothermally-fed combined heat-and-power (CHP) plant coupled to *third* and *fourth* generation thermal networks is investigated. The series and parallel CHP configurations are compared based on an exergy analysis. Whether the series or the parallel CHP has the best performance depends on the thermal network requirements. The results are discussed for a wide range of supply ($40 - 110°C$) and return ($30 - 70°C$) temperatures and for three values of the heat demand. The heat-to-electricity conversion is done via an Organic Rankine Cycle (ORC). In general, the parallel configuration is the most appropriate for the connection to high-temperature thermal networks and the series configuration performs better for the connection to low-temperature thermal networks. For a nominal heat demand of 6MW, the parallel configuration connected to a 80/60 thermal network has an exergetic plant efficiency of 41.25% which is 1.67%-pts higher than for a pure electrical power plant. The corresponding electrical power output is 89% of the pure electrical power plant. The series configuration connected to a 50/30 thermal network has an exergetic efficiency of 42.63%, which is 3.05%-pts higher than for a pure electrical power plant and produces the same electrical power output. An additional important finding is that for isentropic and dry ORC fluids, the use of superheating might increase the electrical power output if the ORC outlet temperature is constrained to a relatively high value. For the investigated brine conditions and R236ea as a working fluid, the use of superheating im-

*Corresponding author
Email address: william.dhaeseleer@kuleuven.be (William D'haeseleer)

proves the electrical power output already for ORC outlet temperatures higher than $80°C$ in case of a recuperated ORC. For the basic cycle, this is only for ORC outlet temperatures higher than $109°C$.

Keywords: low-grade geothermal energy, CHP, ORC, fourth generation thermal networks

1. Introduction

In contrast to the highly intermittent output of wind turbines and PV solar, deep-geothermal energy is a renewable energy source which delivers a constant heat flow to the earth surface. Geothermal electric power production might increase to 1400 TWh per year in 2050, which is 3.5% of the projected global electricity production. Besides, 3.9% of the final energy for heat might be covered [1].

In northwest Europe, deep-geothermal energy sources are mostly low-temperature ($< 150°C$) sources. For these low-temperatures, the binary power plant is the most appropriate [2, 3]. The Organic Rankine Cycle (ORC) is a proven technology for the conversion of low-temperature heat to electricity [4].

ORC's are widely studied in the literature. Walraven et al. [5], Franco [6] and Li et al. [7] have studied the performance of ORC's fed by a low-temperature geothermal source. Walraven et al. [5] optimized the performance of different types of ORC's and of the Kalina cycle for low-temperature ($100–150°C$) geothermal heat sources. Subcritical and transcritical cycles with one or more pressure levels were discussed as well as the effect of turbine-bleeding and a recuperated ORC cycle. They found that transcritical and multi-pressure subcritical ORC's are the best performing cycles and can achieve exergetic plant efficiencies of more than 50%. Franco [6] has studied the ORC performance for a varying turbine inlet temperature and pressure for a low-temperature geothermal energy source of $100–130°C$. He found that recuperated configurations show only minimal performance increase with respect to the basic configuration, but that a (up to 20%) smaller cooling surface area can be obtained. Li et al. [7] have studied the effect of a varying working fluid mass flow rate and the implementation of a recuperator on the efficiency of an ORC using R123. A geothermal source temperature of $130°C$ was considered. For a 6kW output, they found a cycle efficiency for the recuperated cycle of 7.98%, which is 1.83%-points higher than for the basic cycle.

Dai et al. [8] have studied the ORC performance based on low-temperature ($145°C$) waste heat. They optimized a subcritical ORC for 10 different working fluids and found that R236ea gives the highest exergetic efficiency for the investigated conditions. Li et al. [9] have experimentally measured the performance of a 3.5kW ORC for heat source temperatures of 70–$100°C$. They found that the exergy destruction in the evaporator is the largest, followed by the condenser, and that the total exergetic efficiency is around 40%.

The energy sources for ORC applications are not limited to geothermal. Tchanche et al. [10] have presented a review of ORC applications, including thermal solar electricity, solar thermal driven reverse osmosis desalination, solar pond power systems, ocean thermal energy conversion, biomass CHP's, binary geothermal systems and low-grade waste heat recycling. Quoilin et al. [11] have also presented an overview of ORC applications from different sources, including biomass, geothermal, solar and waste heat. Besides, they have discussed the different types of expansion machines, heat exchangers and pumps which can be used in the ORC cycle and the different aspects which influence the choice of the working fluid.

Different ORC working fluids have been studied more thoroughly in [12, 13]. Saleh et al. [12] have performed a thermodynamic screening of 31 pure working fluids for ORC's, using the BACKONE equation of state[1]. Chen et al. [13] have screened 35 working fluids for use in ORC's. They have mentioned the importance of thermodynamic & physical properties, stability, environmental impacts, safety & compatibility, availability and cost as main considerations when selecting the working fluid.

Due to the high drilling costs of deep-geothermal power plants (up to 70% of the investment costs [11]), the overall plant efficiency, and hence the plant economics, might be increased by the combined production of electricity and useful heat. Some research on combined heat-and-power plants has already been done. Rubio-Maya et al. [15] have reviewed the use of low- and medium-enthalpy geothermal sources in cascade manner around the world. They concluded that the use of geothermal energy in cascade improves the resource utilization. Li et al. [16] have compared the

[1] "..., BACKONE is a family of physically based EOS [14], which is able to describe thermodynamic properties of nonpolar, dipolar and quadrupolar fluids with good to excellent accuracy. In BACKONE the Helmholtz energy is written as a sum of contributions from characteristic intermolecular interactions." - citation from [12].

series and parallel configurations of an ORC subsystem, an oil gathering and transportation heat tracing (OGTHT) subsystem and an oil recovery subsystem. The geothermal source temperature was 100–150°C. They found that the series configuration is preferable for high geothermal water inlet temperatures and low heat source inlet temperatures, and just the reverse for the parallel configuration. Heberle et al. [4] have compared the series and parallel configurations of an ORC and heat delivery to a district heating (DH) system by second-law analysis. They found that the series configuration is the most efficient concept. Geothermal resources at a temperature level below 450K were considered and the DH system supply and return temperatures were 75°C and 50°C, respectively. Habka and Ajib [17] have compared the performance of the parallel, the series and the "Glewe" configuration for a geothermal source of 100°C. The "Glewe" configuration is based on a series configuration of the ORC and the DH system. But part of the brine flow rate bypasses the ORC and mixes with the ORC outlet stream to increase the brine temperature which enters the heat exchanger of the DH system. Supply temperatures in the range of 60–90°C for the DH system and heat demands of 110–150kW were considered. The comparison between the CHP plants has shown that the parallel configuration is more economic and the series configuration is energetically more efficient, while the integration according to Glewe-plant does not provide significant performance improvements. Habka and Ajib [18], furthermore, have proposed 4 new configurations for a geothermally-fed CHP plant. They have compared net power consumption and exergetic plant efficiency with the series and parallel CHP configurations and with the ORC stand-alone plant. The working fluid was R134a. Geothermal water at 100°C and a flow rate of 1kg/s were assumed and heat was delivered to a DH system with supply and return temperatures of 75°C and 50°C, respectively, and a heat demand of 110–170kW. For the investigated boundary conditions, the optimized cycles and also the series plant have better energetic performance than the parallel plant. All CHP configurations have higher exergetic efficiency, while the stand-alone plant produces more electricity.

In this paper, a low-temperature ($T = 130°C$) geothermally-fed CHP plant is considered, which provides heat to a DH system. Current state-of-the-art DH systems are third generation thermal networks, with typical supply temperatures of 70–110°C. However, future energy systems are likely to integrate renewables, (e.g. deep-geothermal) CHP production, low-energy buildings and low-temperature DH networks to go towards a more sustainable and integrated energy system. Supply temperatures may go down to 40°C [19]. The connection to third generation thermal networks has

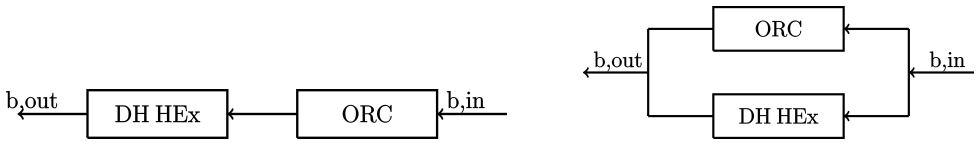

(a) Series (b) Parallel

Figure 1: Series and parallel CHP configurations.

already been studied in the literature, the connection to fourth generation thermal networks is new. Two CHP configurations are investigated, which are schematically presented in Figure 1. For the series configuration, the brine (geothermal water) delivers heat to the ORC at high temperature and subsequently to the DH system at a lower temperature. For the parallel configuration, heat is delivered to both the DH system and the ORC at a high temperature but at a lower flow rate. The goal is to compare the performance of the series and parallel configurations based on an exergy analysis. Rather than focusing on a single DH system, the optimal CHP configuration are determined for every combination of T_{supply} in $40 - 110°C$ and T_{return} in $30 - 70°C$. As a case study, the results for a typical third generation 80/60 and fourth generation 50/30 DH system will be discussed more in detail. In addition, also the usefulness of a recuperator will be discussed and we will indicate that the use of superheating for dry/isentropic working fluids might improve the electrical power output for sufficiently high ORC outlet temperatures.

2. Methodology

First, the objectives and constraints are stated, followed by the models and assumptions and the most important exergy concepts. Finally, the models are verified against modern literature.

2.1. Objectives and constraints

The objective is to maximize the electricity production of the ORC while satisfying a given heat demand of the DH system. No additional boilers or storage facilities are considered.

The net electric power $\dot{W}_{net}$ produced by the **ORC** is:

$$\dot{W}_{net} = \dot{W}_t \eta_g - \frac{\dot{W}_p}{\eta_m} \tag{1}$$

with $\dot{W}_t$ the turbine power, $\dot{W}_p$ the pump power, η_g the electric generator efficiency and η_m the electric motor efficiency.

The **brine** temperature and pressure are $T_{b,in} = 130°C$ and $p_{b,in} = 40bar(a)$, according to the expected brine conditions in Flanders [20]. The brine flow rate is $\dot{m}_b = 194kg/s$.

We investigate the connection to third and fourth generation thermal networks, with imposed supply $(40 - 110°C)$ and return $(30 - 70°C)$ temperatures and a heat demand which has always to be satisfied.

2.2. Models and assumptions

Figure 2a shows a detailed presentation of a basic ORC. The ORC working fluid is subsequently pressurized by the pump $(1 \rightarrow 2)$, evaporated in the evaporator $(2 \rightarrow 3)$, expanded in the turbine $(3 \rightarrow 4)$ for generating mechanical (and consequently electric) power, and finally condensed back to the original liquid state in the condenser $(4 \rightarrow 1)$. Figure 2b shows the corresponding T-s diagram.

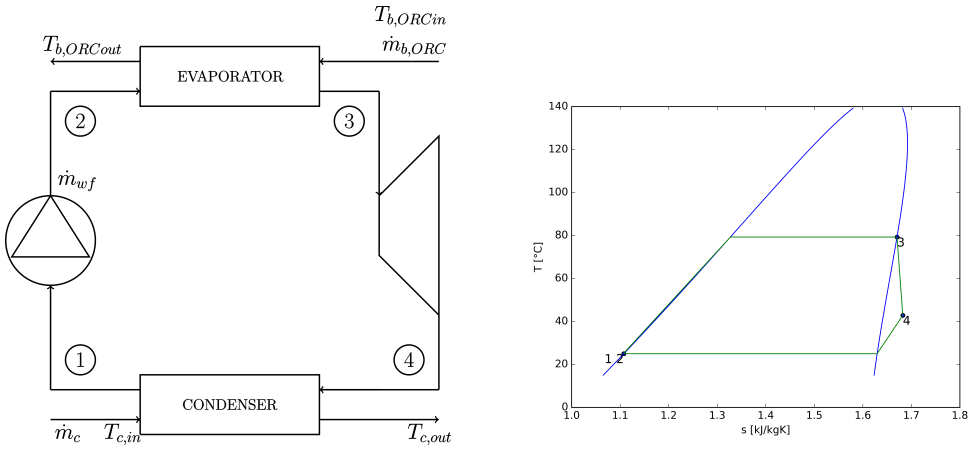

(a) Basic ORC

(b) T-s diagram

Figure 2: Basic ORC and T-s diagram with indication of the nomenclature.

Heat transfer in the evaporator is modeled as follows:

$$\dot{Q}_{ORC} = \dot{m}_{b,ORC}(h_{b,ORCin} - h_{b,ORCout}) \tag{2}$$

$$\dot{Q}_{ORC} = \dot{m}_{wf}(h_3 - h_2) \tag{3}$$

with $\dot{Q}_{ORC}$ the heat addition to the ORC, $\dot{m}_{b,ORC}$ the brine flow rate in the ORC branch and $\dot{m}_{wf}$ the working fluid mass flow rate. $h_{b,ORCin}$ and $h_{b,ORCout}$ are the specific enthalpies of the brine at the ORC inlet and outlet, respectively, h_2 and h_3 the specific enthalpies of the working fluid at state 2 and 3. Other heat exchangers are modeled in a similar way.

The pump and turbine powers are calculated by:

$$\dot{W}_p = \dot{m}_{wf}(h_2 - h_1) \tag{4}$$

$$\dot{W}_t = \dot{m}_{wf}(h_3 - h_4) \tag{5}$$

The relation between inlet and outlet state for the pump and turbine are found using the corresponding isentropic efficiencies:

$$\eta_p = \frac{h_{2s} - h_1}{h_2 - h_1} \tag{6}$$

$$\eta_t = \frac{h_4 - h_3}{h_{4s} - h_3} \tag{7}$$

Subscript s refers to the isentropic state.

Mixing of two streams (only for the parallel configuration) is modeled by:

$$\dot{m}_b h_{b,out} = \dot{m}_{b,ORC} h_{b,ORCout} + \dot{m}_{b,DH} h_{b,DHout} \tag{8}$$

$$\dot{m}_b = \dot{m}_{b,ORC} + \dot{m}_{b,DH} \tag{9}$$

with $\dot{m}_{b,DH}$ the brine mass flow rate through the DH branch, $h_{b,DHout}$ the brine specific enthalpy at the DH outlet and $h_{b,out}$ the remaining specific enthalpy of the brine.

The fixed parameter values are given in Table 1. ΔT_{pinch} is the pinch-point-temperature difference in the heat exchangers, the subscripts ref and c, in indicate the reference state and the cooling water inlet state, respectively. Furthermore, kinetic and potential energy differences are neglected, and we do not consider pressure drops in the heat exchangers.

R236ea is investigated as the working fluid. Amongst others, according to [8, 13], no superheating is required for this isentropic working fluid. However, a small degree of superheating $\Delta T_{sup} =$

parameter	values	parameter	values
T_1	$25°C$	η_m	98%
ΔT_{pinch}	$5°C$	T_{ref}	$15°C$
η_p	80%	p_{ref}	1bar(a)
η_t	85%	$T_{c,in}$	$15°C$
η_g	98%	$p_{c,in}$	2bar(a)

Table 1: Fixed model parameters [5, 21].

	MW [g/mol]	$T_{crit}[°C]$	p_{crit} [bar(a)]	ODP	GWP	atmospheric lifetime [years]
R236ea	152.04	139.3	35.0	0	1410	11
R123	152.93	183.7	36.6	0.010	77	1.3
R600a	58.12	134.7	36.3	0	20	0.016
R245fa	134.05	154.0	36.5	0	1050	7.7

Table 2: Thermodynamic and environmental parameters of ORC working fluids [22].

$0.01°C$ is considered to get numerical stability. The thermodynamic and environmental properties of R236ea are given in Table 2 [22]. Additionally, the properties of the working fluids which have been used in the validation (Table 3) are also given in Tabel 2.

2.3. Exergy analysis

The CHP plant has two useful outputs, electric power and thermal power (for short referred to as "heat") which is delivered to the DH system. Taking into account the quality of heat, the thermal cycle efficiency and the brine utilization, the exergetic plant efficiency η_{ex} is the most appropriate performance indicator to compare different CHP configurations:

$$\eta_{ex} = \frac{\dot{E}x_{DH} + \dot{W}_{net}}{\dot{E}x_{b,in}} \tag{10}$$

The brine inlet flow exergy $\dot{E}x_{b,in}$ and the DH flow exergy $\dot{E}x_{DH}$ are defined as follows:

$$\dot{E}x_{b,in} = \dot{m}_b ex_{b,in} \tag{11}$$

$$\dot{E}x_{DH} = \dot{m}_{DH}\left[ex_{supply} - ex_{return}\right] \tag{12}$$

with $\dot{m}_b$ and $\dot{m}_{DH}$ the brine and DH system mass flow rates, and the subscripts *supply* and $return$ refer to the supply and return states of the DH system. The specific flow exergy ex is the maximal specific work the fluid can deliver with respect to the environment, and is generally defined as:

$$ex = (h - h_{ref}) - T_{ref}(s - s_{ref}) \tag{13}$$

with T, h and s the temperature, specific enthalpy and specific entropy and subscript ref refers to the reference state of the environment.

2.4. Model validation

The models are implemented in Python [23]. CasAdi [24] is used as a dynamic optimization framework. The maximal net electrical power output is found by means of a derivative-based optimization using the IpOpt solver [25] for solving the non-linear problem. Fluid properties are called from the REFPROP 8.0 database [26].

The ORC model is validated against the results obtained by Dai et al. [8], Walraven et al. [5] and Saleh et al. [12] for the respective conditions. Saleh et al. use the BACKONE equation of state for the calculation of fluid properties whereas the other references use the REFPROP database. The results are summarized in Table 3 and are very close. $\eta_{en} = \frac{\dot{W}_{net}}{\dot{Q}_{ORC}}$ and $w = \frac{\dot{W}_{net}}{\dot{m}_{wf}}$ are the energetic cycle efficiency and the net specific work, respectively.

The ORC cycle, and the parallel and series configuration models are additionally validated against the results of Habka et al. [17] for the respective conditions. The net electric power generation for each of these configurations is compared to the result of our own models (values between brackets). The results are 15.45kW (15.18kW) for the ORC cycle, 3.19kW (3.08kW) for the parallel and 4.36kW (4.20kW) for the series configuration. All errors are within 3.7%, so we can conclude that the accuracy of our models is satisfying.

3. Results

First, the performance of the pure electrical power plant is discussed. The performance of the parallel and the series configurations are discussed subsequently. The performance of the CHP

T_{evap} [°C]	p_{evap} [bar]	$T_{b,out}$ [°C]	η_{en} [%]	w [kJ/kg wf]	working fluid	source
87.73	12.0	59.59	11.53	22.71	R236ea	[8]
87.28	11.9	59.57	11.48	22.57	R236ea	[5]
87.28	11.9	59.44	11.48	22.57	R236ea	present
83.23	5.3	68.10	11.83	24.25	R123	[8]
83.00	5.3	68.02	11.80	24.18	R123	present
100	15.74	-	12.02	24.18	R236ea	[12]
100	15.72	-	12.04	23.74	R236ea	present
100	19.98	-	12.12	48.96	R600a	[12]
100	19.86	-	12.12	48.62	R600a	present
100	12.67	-	12.52	29.92	R245fa	[12]
100	12.64	-	12.60	29.47	R245fa	present

Table 3: Validation of the ORC model against modern literature.

configurations is given as a function of the DH system temperatures (T_{supply} and T_{return}). Multiple (but constant) values of the heat demand are considered: $\dot{Q}_{DH} = 3MW$, $\dot{Q}_{DH} = 6MW$ and $\dot{Q}_{DH} = 9MW$. Afterwards, as a case study, we elaborate more in detail on the results for the connection to two typical types of thermal networks. A state-of-the-art third generation thermal network with $T_{supply} = 80°C$ & $T_{return} = 60°C$ [27] and a (future) fourth generation thermal network with $T_{supply} = 50°C$ & $T_{return} = 30°C$ [28]. These are also referred to as high- and low-temperature DH systems, respectively. In the discussion of the series CHP configuration we make a small side-trip to the usefulness of a recuperator. Finally, we compare the performance of the series and the parallel CHP configurations for every set of T_{supply}, T_{return} and $\dot{Q}_{DH}$.

3.1. Pure electrical power plant

For the pure electrical power plant, no district heating system is considered and only electrical power is generated by means of an Organic Rankine Cycle (ORC), which was already presented in Figure 2a. Figure 2b shows the corresponding T-s diagram for the optimal cycle operation for the investigated brine conditions. The pure electrical power plant has an electrical power output of $\dot{W}_{net} = 6.18MW$ and an exergetic plant efficiency of $\eta_{ex} = 39.58\%$. The parallel and series CHP

performances will be compared with the performance of this pure electrical power plant.

3.2. Parallel configuration

First the performance of the parallel configuration is discussed as a function of the thermal network requirements. Afterwards, the connection to a typical third and fourth generation thermal network is discussed more in detail.

3.2.1. Performance for imposed DH system requirements

Figure 3 shows the electrical power output of the parallel CHP configuration as a function of the supply and return temperatures, and for three values of the heat demand. Supply and return temperatures in the range of $40-110°C$ and $30-70°C$ are considered, respectively. Besides, a low heat demand of $\dot{Q}_{DH} = 3MW$, a medium heat demand of $\dot{Q}_{DH} = 6MW$ and a high heat demand of $\dot{Q}_{DH} = 9MW$ are investigated.

Going from Figure 3a to Figure 3c, we see that the electrical power output decreases for a higher heat demand of the DH system. Since a higher heat demand requires a higher brine mass flow rate through the DH HEx $\dot{m}_{b,DH}$ (see Figure 1), the brine mass flow rate through the ORC branch $\dot{m}_{b,ORC}$ decreases. As a direct consequence, the heat addition to the ORC is lower and also the electrical power output $\dot{W}_{net}$ decreases.

If we consider a constant heat demand, e.g. Figure 3b, we see that $\dot{W}_{net}$ does not depend on the supply temperature T_{supply}. Furthermore, also the influence of the return temperature T_{return} is presented. Consider again Figure 3b, the higher the return temperature T_{return}, the higher the brine mass flow rate through the DH HEx $\dot{m}_{DH}$ should be to satisfy the constant heat demand of 6MW. As a result, the brine flow rate through the ORC branch $\dot{m}_{b,ORC}$ is lower and hence $\dot{W}_{net}$ decreases with the return temperature.

3.2.2. Case study: Typical third and fourth generation DH systems

The performance results for the connection to a third generation (80/60) and a fourth generation (50/30) thermal network are summarized in Table 4. An important characteristic of the parallel

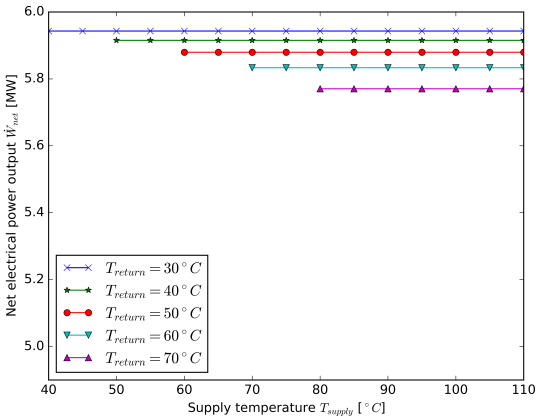

(a) $\dot{Q}_{DH} = 3MW$

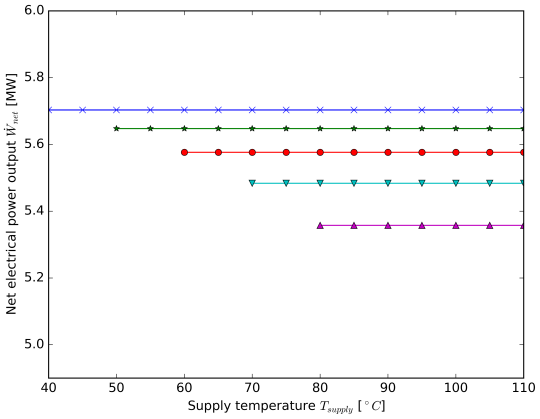

(b) $\dot{Q}_{DH} = 6MW$

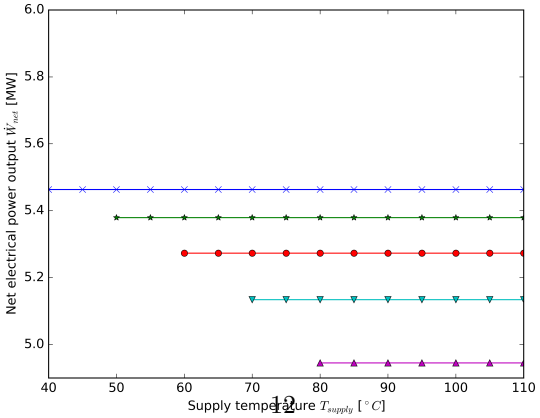

(c) $\dot{Q}_{DH} = 9MW$

Figure 3: Electrical power output of the parallel CHP configuration as a function of the DH system requirements.

T_{supply}/T_{return} [°C]	$\dot{Q}_{DH}$ [MW]	$T_{b,out}$ [°C]	$T_{b,ORCout}$ [°C]	$\dot{Q}_b$ [MW]	$\dot{W}_{net}$ [MW]	η_{ex} [%]
80/60	3	57.59	57.15	59.06	5.83	40.41
	6	58.03	57.15	58.71	5.48	41.25
	9	58.48	57.15	58.34	5.13	42.08
50/30	3	56.29	57.15	60.12	5.94	39.57
	6	55.43	57.15	60.81	5.70	39.56
	9	54.57	57.15	61.51	5.46	39.55

Table 4: Performance of the parallel configuration for connection to a third generation 80/60 and a fourth generation 50/30 thermal network, and for multiple values of the heat demand.

configuration is that the optimal ORC outlet temperature $T_{b,ORCout}$ is independent of the DH system requirements and equal to the optimal $T_{b,ORCout}$ for a pure electrical power plant. Furthermore, the trends are different for the high- and low-temperature DH systems.

Consider the 80/60 DH system first:

$$\begin{aligned}
&\dot{Q}_{DH} \nearrow \;\rightarrow\; \dot{m}_{b,DH} \nearrow \;\&\; \dot{m}_{b,ORC} \searrow \\
&\qquad \text{due to } \dot{m}_{b,ORC} \searrow \rightarrow\; \dot{W}_{net} \searrow \\
&\qquad \text{due to } \dot{m}_{b,DH} \nearrow, \dot{m}_{b,ORC} \searrow \;\&\; T_{b,DHout} > T_{b,ORCout} \;\rightarrow\; T_{b,out} \nearrow \\
&\qquad T_{b,out} \nearrow \text{ so } (T_{b,in} - T_{b,out}) \searrow \rightarrow\; \dot{Q}_b \searrow
\end{aligned}$$

Consider now the 50/30 DH system:

$$\begin{aligned}
&\dot{Q}_{DH} \nearrow \;\rightarrow\; \dot{m}_{b,DH} \nearrow \;\&\; \dot{m}_{b,ORC} \searrow \\
&\qquad \text{due to } \dot{m}_{b,ORC} \searrow \rightarrow\; \dot{W}_{net} \searrow \\
&\qquad \text{due to } \dot{m}_{b,DH} \nearrow, \dot{m}_{b,ORC} \searrow \;\&\; T_{b,DHout} < T_{b,ORCout} \;\rightarrow\; T_{b,out} \searrow \\
&\qquad T_{b,out} \searrow \text{ so } (T_{b,in} - T_{b,out}) \nearrow \rightarrow\; \dot{Q}_b \nearrow
\end{aligned}$$

η_{ex} has two contributions: the net electric power and the DH heat flow exergy. For a high-
195 temperature DH system, the temperature of the heat is high enough to compensate for the loss in $\dot{W}_{net}$, so overall $\eta_{ex} \nearrow$. However, for the low-temperature DH system, the lower exergy of low-temperature heat cannot compensate the smaller $\dot{W}_{net}$ and $\eta_{ex} \searrow$. Whether $T_{b,DHout} > T_{b,ORCout}$

or $T_{b,DHout} < T_{b,ORCout}$ determines the trend for the brine outlet temperature $T_{b,out}$, the brine heat extraction $\dot{Q}_b$ and the exergetic plant efficiency η_{ex}. This condition is determined by the DH system return temperature: $T_{b,DHout} \geq T_{return} + \Delta T_{pinch}$.

Finally, we compare the performance for connection to a high- and a low-temperature DH system at a constant heat demand $\dot{Q}_{DH} = const$ (e.g. $\dot{Q}_{DH} = 6MW$):

$$\begin{aligned} \text{for } 80/60 \rightarrow 50/30 \text{ and } \dot{Q}_{DH} = const \;\; &\rightarrow \;\; T_{b,DHout} \searrow \text{ due to } T_{return} \searrow \\ &\rightarrow \;\; (T_{b,DHin} - T_{b,DHout}) \nearrow \rightarrow \;\; \dot{m}_{b,DH} \searrow \;\; \& \;\; \dot{m}_{b,ORC} \nearrow \\ &\text{due to } \dot{m}_{b,ORC} \nearrow \rightarrow \;\; \dot{W}_{net} \nearrow \end{aligned}$$

More net electric power is produced for the connection to a low-temperature thermal network, but the exergetic plant efficiency is lower due to the lower quality of low-temperature heat.

With respect to the pure electrical power plant, the electrical power output is always lower due to the lower heat addition to the ORC. However, the exergetic plant efficiency is higher in case of the connection to a (high-temperature) third generation thermal network.

3.3. Series configuration

First the performance of the series configuration is discussed as a function of the thermal network requirements. Afterwards, the connection to a typical third and fourth generation thermal network is discussed more in detail. Both, the implementation of a basic and a recuperated ORC are considered and the usefulness of a recuperator is explained.

3.3.1. Performance for imposed DH system requirements

Figure 4 shows the electrical power output of the series CHP configuration as a function of the supply and return temperatures, and for three values of the heat demand. As for the parallel configuration, supply and return temperatures in the range of $40 - 110°C$ and $30 - 70°C$ are considered, respectively. Besides, a low heat demand of $\dot{Q}_{DH} = 3MW$, a medium heat demand of $\dot{Q}_{DH} = 6MW$ and a high heat demand of $\dot{Q}_{DH} = 9MW$ are investigated.

Going from Figure 4a to Figure 4c, we see that the electrical power output is independent of the heat demand of the DH system. Since the entire brine mass flow rate passes the ORC, the heat delivery to the ORC and hence the electrical power output is the same.

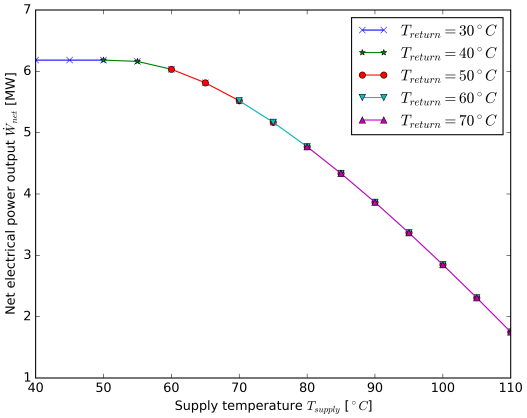

(a) $\dot{Q}_{DH} = 3MW$

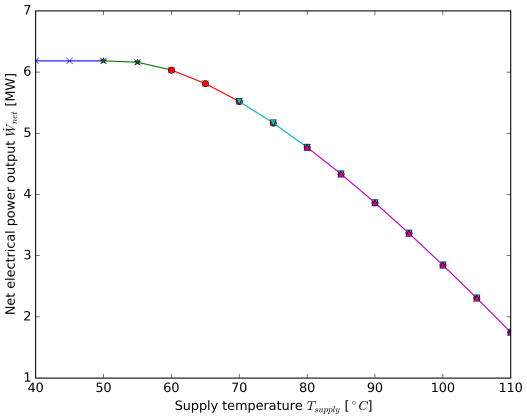

(b) $\dot{Q}_{DH} = 6MW$

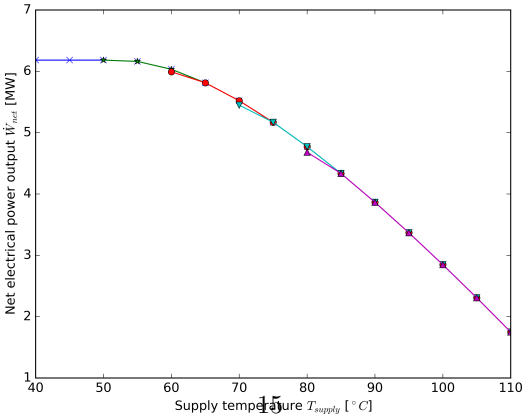

(c) $\dot{Q}_{DH} = 9MW$

Figure 4: Electrical power output of the series CHP configuration as a function of the DH system requirements.

If we consider a constant heat demand, e.g. Figure 4b, we see that $\dot{W}_{net}$ depends on T_{supply}. Up to $T_{supply} = 57.15°C$, the electrical power output $\dot{W} = 6.18MW$ equals the electrical power output of the pure electrical power plant. For $T_{supply} > 57.15°C$, the ORC heat addition is constrained by the supply temperature of the DH system. The pinch-point-temperature difference $\Delta T_{pinch} = 5°C$ is located at the supply side of DH Hex and $T_{b,ORCout} = T_{supply} + \Delta T_{pinch}$. Furthermore, in general, $\dot{W}_{net}$ does not depend on the return temperature. However, for high heat demands the power output might be constrained by T_{return}. Consider Figure 4c for the high heat demand of $\dot{Q}_{DH} = 9MW$. For low temperature differences $T_{supply} - T_{return}$ and high values of T_{return}, the brine is cooled down until the pinch-point-temperature difference is reached at the return side of DH HEx. The pinch-point-location shifts from the supply side to the return side of DH HEx. As a result, the ORC outlet temperature $T_{b,ORCout}$ is higher and the ORC heat addition – and hence $\dot{W}_{net}$ – is lower. This reflects in the *spikes* in Figure 4c. For $T_{supply} - T_{return} = 10°$ and $T_{return} \geq 50°C$, $\dot{W}_{net}$ is slightly lower than the general curve.

3.3.2. The usefulness of a recuperator

The recuperated ORC has an extra heat exchanger in comparison to the basic cycle. The *recuperator* allows internal heat recuperation in the ORC, thereby increasing the cycle efficiency. This is illustrated on the basis of Figure 5.

In the recuperator, the temperature of the turbine outlet vapor is reduced from (4) to (4recup), and the temperature of the liquid at the pump outlet is increased from (2) to (2recup). In the T-s diagram of Figure 5b, (1)→(4recup) represents the specific cooling power, which is smaller than (1)→(4) for the basic ORC. (2recup)→(3) represents the specific heat addition by the brine, which is also smaller than (2)→(3) for the basic ORC. The same specific turbine power (3)→(4) can be generated for a smaller specific brine heat addition such that the cycle efficiency is higher for the recuperated ORC in comparison to the basic ORC.

The implementation of a recuperator is only useful in case of a constrained ORC outlet temperature $T_{b,ORCout}$. In case of the parallel configuration, the ORC outlet temperature is independent of the DH system requirements (which can be seen in Table 4). The implementation of a recuperated ORC instead of the basic one would lead to the same electrical power output but would introduce an extra component (cost). Therefore, we choose for the basic ORC implementation for the parallel set-up.

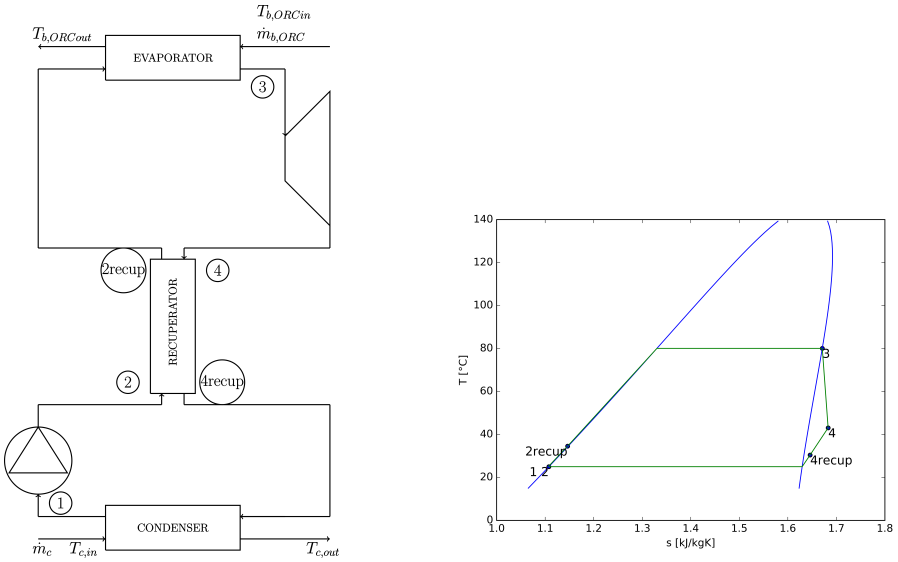

(a) Recuperated ORC

(b) T-s diagram

Figure 5: Recuperated ORC and T-s diagram with indication of the states.

However, in case of the series configuration, the ORC outlet temperature is constrained by T_{supply} for $T_{supply} \geq 57.15°C$, which was explained by means of Figure 4. Therefore, the recuperated ORC performs better for $T_{supply} \geq 57.15°C$. Due to the internal heat recuperation in the recuperator, the electrical power output is higher for the same ORC heat addition.

3.3.3. Case study: Typical third and fourth generation DH systems

The performance results for the connection to a third generation (80/60) and a fourth generation (50/30) thermal network are summarized in Table 5. Both, the results for a basic and a recuperated ORC implementation are given. In contrast to the parallel configuration, $T_{b,ORCout}$ is influenced by the DH system requirements in case of high-temperature DH systems.

T_{supply}/T_{return} [°C]	$\dot{Q}_{DH}$ [MW]	$T_{b,out}$ [°C]	$T_{b,ORCout}$ [°C]	$\dot{Q}_b$ [MW]	$\dot{W}_{net}$ [MW]	η_{ex} [%]
80/60	3	81.31	85	39.82	4.77	33.62
basic ORC	6	77.62	85	42.82	4.77	36.69
	9	73.92	85	45.82	4.77	39.76
80/60	3	81.31	85	39.82	5.10	35.69
recuperated ORC	6	77.62	85	42.82	5.10	38.77
	9	73.92	85	45.82	5.10	41.84
50/30	3	53.44	57.15	62.42	6.18	41.10
basic ORC	6	49.74	57.15	65.42	6.18	42.63
	9	46.03	57.15	68.42	6.18	44.16
50/30	3	58.48	62.18	58.34	6.18	41.10
recuperated ORC	6	54.78	62.18	61.34	6.18	42.63
	9	51.07	62.18	64.34	6.18	44.15

Table 5: Performance of the series configuration with basic ORC and recuperated ORC for connection to a third generation 80/60 and a fourth generation 50/30 thermal network, and for multiple values of the heat demand.

For the high-temperature DH system:

$$
\begin{aligned}
T_{b,ORCout} &= T_{supply} + \Delta T_{pinch} \\
T_{b,ORCout} = const \;&\rightarrow\; (T_{b,ORCin} - T_{b,ORCout}) = const \;\rightarrow\; \dot{W}_{net} = const \\
\dot{Q}_{DH} \nearrow \;&\rightarrow\; T_{b,DHout} = T_{b,out} \searrow \\
&\rightarrow\; (T_{b,in} - T_{b,out}) \nearrow \rightarrow\; \dot{Q}_b \nearrow \\
&\rightarrow\; \dot{W}_{net} = const \;\&\; \dot{Q}_{DH} \nearrow \rightarrow\; \eta_{ex} \nearrow
\end{aligned}
$$

For low-temperature DH systems, $T_{b,ORCout}$ is not constrained by T_{supply}. The optimal $T_{b,ORCout}$ is the same as for a pure electrical power plant. The trends are similar to those of the high-temperature DH system.

When comparing the performance of the high-temperature to the low-temperature DH system for

a constant heat demand $\dot{Q}_{DH} = const$ (e.g. $\dot{Q}_{DH} = 6MW$):

$$\begin{aligned} \text{for } 80/60 \rightarrow 50/30 \text{ and } \dot{Q}_{DH} = const \;\; &\rightarrow \;\; T_{b,ORCout} \searrow \text{ due to } T_{supply} \searrow \\ &\rightarrow \;\; (T_{b,ORCin} - T_{b,ORCout}) \nearrow \rightarrow \;\; \dot{W}_{net} \nearrow \end{aligned}$$

More net electric power is produced for the connection to a low-temperature thermal network. Also the exergetic plant efficiency is higher due to the significantly higher $\dot{W}_{net}$.

When comparing the results of the series CHP with basic ORC with the results for the recuperated ORC implementation, we see that the optimal ORC outlet temperature is different. Due to the internal heat recovery, the optimal ORC outlet temperature of the recuperated ORC is $T^{opt}_{b,ORCout} = 62.18°C$, which is higher than $T^{opt}_{b,ORCout} = 57.15°C$ for the basic ORC. For the low-temperature DH system, as a result, the brine heat extraction $\dot{Q}_b$ is lower and the brine injection temperature $T_{b,out}$ is higher in case of the recuperated ORC. Since the electrical power output is the same, also the exergetic plant efficiency is equal for a certain heat demand. For the high-temperature DH system, on the contrary, the ORC outlet temperature is constrained by T_{supply} which leads to equal values for the brine heat extraction and brine injection temperature. Due to the recuperator, the electrical power output of the recuperated ORC is higher for the same heat demand, such that also the exergetic plant efficiency is higher for the recuperated series CHP.

3.4. Parallel versus series configuration

First the performance of the series and parallel configurations are given as a function of the thermal network requirements. From the summarizing figures, we can derive whether the parallel or the series configuration has the best performance for the connection to a thermal network with imposed requirements for the supply and return temperatures and for the heat demand. Afterwards, we give conclusions for the connection to a typical third and fourth generation thermal network.

3.4.1. Performance for imposed DH system requirements

The goal has been to indicate the CHP configuration with the best performance for the connection to a (state-of-the-art) high-temperature DH system or to a (future) low-temperature DH system. Figure 6 is summarizing the performance of the series and parallel CHP configurations for the connection to a DH system with imposed supply & return temperatures and heat demand. Supply

and return temperatures in the range of $40-110°C$ and $30-70°C$ are considered, respectively, and a low ($\dot{Q}_{DH} = 3MW$), a medium ($\dot{Q}_{DH} = 6MW$) and a high ($\dot{Q}_{DH} = 9MW$) heat demand are investigated. The electrical power output of the pure electrical power plant is given by the black line (at $\dot{W}_{net} = 6.18MW$).

We conclude that the parallel CHP has the best performance for the connection to a high-temperature DH system and the series CHP configuration is more appropriate for the connection to a low-temperature thermal network. Heat is directly delivered to the DH system at high temperature in case of the parallel configuration, whereas the series configuration can keep a high electrical power output when connected to a low-temperature DH system. Furthermore, from Figure 6 follows that higher values of the heat demand are in favor of the series configuration.

3.4.2. Case study: Typical third and fourth generation DH systems

The parallel configuration has the highest electrical power output for the connection to the considered (high-temperature) third generation thermal network whereas the series configuration has the best performance for the connection to the considered (low-temperature) fourth generation thermal network. For a heat demand of $\dot{Q}_{DH} = 6MW$, the parallel configuration connected to the 80/60 DH system produces $\dot{W}_{net} = 5.48MW$ of net electric power and has an exergetic plant efficiency of $\eta_{ex} = 41.25\%$. The series configuration connected to the 50/30 DH system produces $\dot{W}_{net} = 6.18MW$ of net electric power and has an exergetic plant efficiency of $\eta_{ex} = 42.63\%$. Because there is no limit on the ORC outlet temperature, the ORC power generation for the series configuration connected to the low-temperature (50/30) DH system produces as much electric power as a pure electrical power plant. However, the exergetic plant efficiency is increased from $\eta_{ex} = 39.58\%$ to $\eta_{ex} = 42.63\%$ by making use of the "ORC waste heat". For the parallel configuration, the power production is lower due to the lower heat delivery to the ORC ($\dot{m}_{b,ORC} < \dot{m}_b$), but the exergetic plant efficiency is higher than for a pure electrical power plant: $\eta_{ex} = 41.25\%$ versus $\eta_{ex} = 39.58\%$. Hereby, we prove that in both cases the optimal CHP plant has a higher exergetic plant efficiency than the pure electrical power plant. So, combined heat-and-power production might increase the overall plant economics.

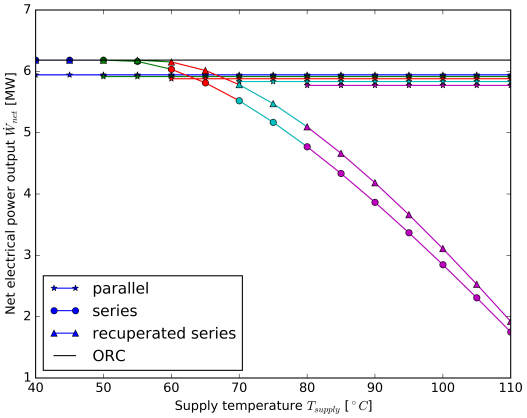

(a) $\dot{Q}_{DH} = 3MW$

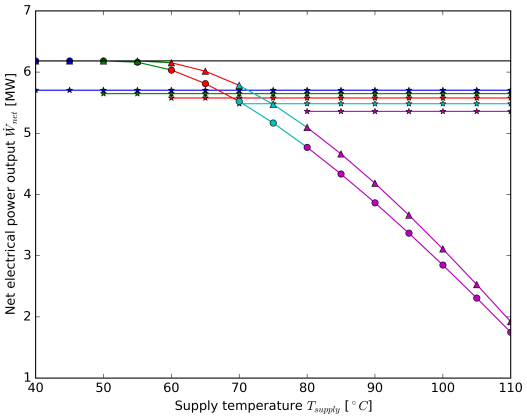

(b) $\dot{Q}_{DH} = 6MW$

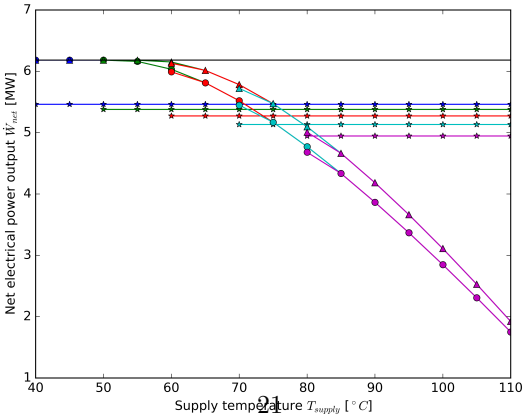

(c) $\dot{Q}_{DH} = 9MW$

Figure 6: Electrical power output of the parallel and the series CHP configurations as a function of the DH system requirements.

4. Discussion on the degree of superheating

The above results have been performed based on the assumption of no superheating ($\Delta T_{sup} = 0.01°C$ for numerical stability). However, we have found that superheating might be of interest for this isentropic (slightly dry) working fluid R236ea. A degree of superheating greater than zero might improve the electrical power production of the ORC in case of a constrained ORC outlet temperature $T_{b,ORCout}$. For the basic ORC, $T_{b,ORCout}$ should be higher than $109°C$, but for the recuperated ORC, the performance might be improved for much lower values of the ORC outlet temperature, i.e. for $T_{b,ORCout} \geq 80°C$. For example, this means that the performance of the recuperated series configuration for the connection to a DH system with $T_{supply} \geq 75°C$ might be improved by using superheating.

Figure 7 shows the T-s and T-Q diagrams for the recuperated ORC with $T_{b,ORCout} = 80°C$, $T_{b,ORCout} = 85°C$ and $T_{b,ORCout} = 90°C$. It is clear that for a more stringent constraint on the ORC outlet temperature, the recuperator is more useful. Furthermore, by increasing the degree of superheating, there is a better match of the heating curve of the working fluid with the brine cooling curve in the T-Q diagram. Therefore, the electrical power output can be increased by using superheating $\Delta T_{sup} > 0°C$.

Additionally, Figure 8 shows the electrical power output of the recuperated ORC, the turbine inlet temperature and the usefulness of the recuperator as a function of the degree of superheating, and for several values of the ORC outlet temperature $T_{b,ORCout}$. It follows from figure 8a that for $T_{b,ORCout} = 75°C$, the maximal electrical power output corresponds to a superheating of $0°C$. However for $T_{b,ORCout} \geq 80°C$, the maximal electrical power output has $\Delta T_{sup} > 0°C$. Furthermore, a *kink* shows up in some curves for the electrical power output. At the degree of superheating where this *kink* occurs, the pinch-point-temperature of the evaporator shifts to the brine inlet side. This can be seen in Figure 8b because at the degree of superheating which corresponds to the *kink* in the $\dot{W}_{net}$-curve, the turbine inlet temperature reaches the temperature of $T_{b,in} - \Delta T_{pinch} = 125°C$. Finally, from Figure 8c it follows that the recuperator efficiency increases with the degree of superheating which was expected. From the T-s diagrams of Figure 7 it follows that the turbine outlet temperature increases with the degree of superheating, such that there is more potential for heat recovery. In Figure 8c, we see that the curves for the recuperator efficiency for multiple values of $T_{b,ORCout}$ coincide from the degree of superheating at the *kink*. From the degree of superheating

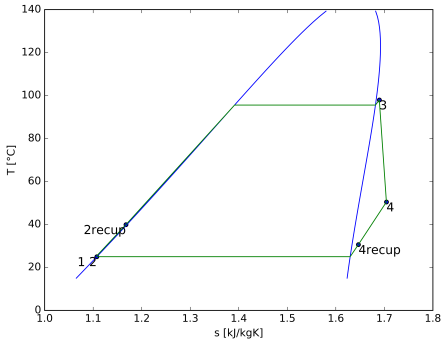

(a) T-s diagram: $T_{b,ORCout} = 80°C$

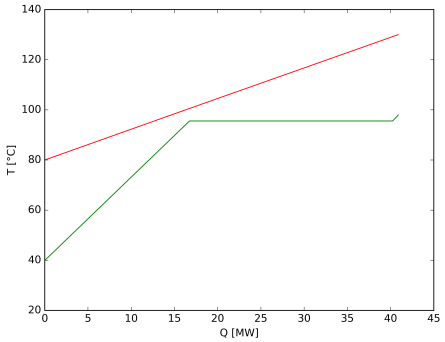

(b) T-Q diagram: $T_{b,ORCout} = 80°C$

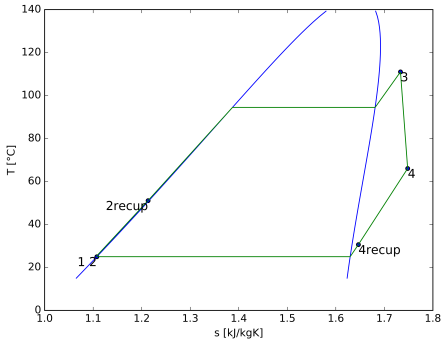

(c) T-s diagram: $T_{b,ORCout} = 85°C$

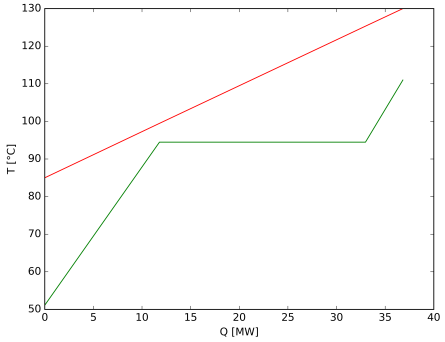

(d) T-Q diagram: $T_{b,ORCout} = 85°C$

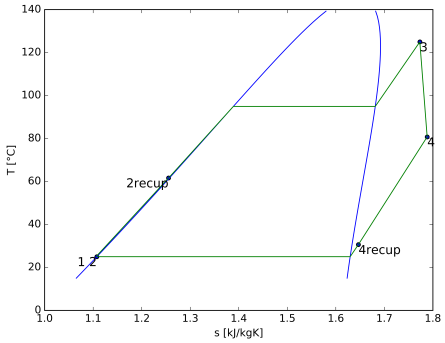

(e) T-s diagram: $T_{b,ORCout} = 90°C$

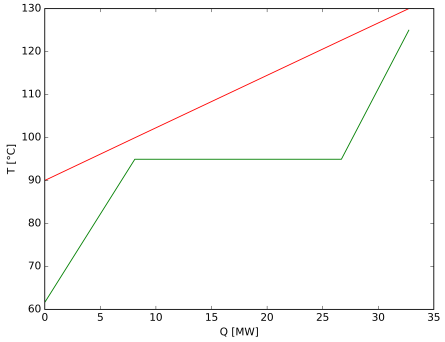

(f) T-Q diagram: $T_{b,ORCout} = 90°C$

Figure 7: T-s and T-Q diagrams for the recuperated ORC for a constrained ORC outlet temperature.

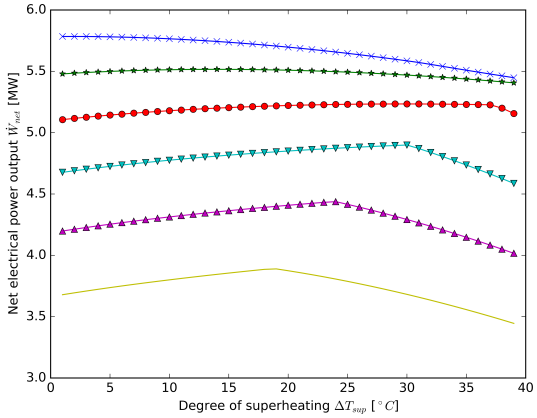

(a) Electrical power output

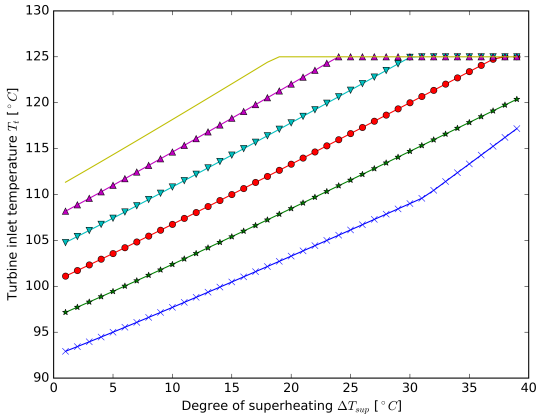

(b) Turbine inlet temperature

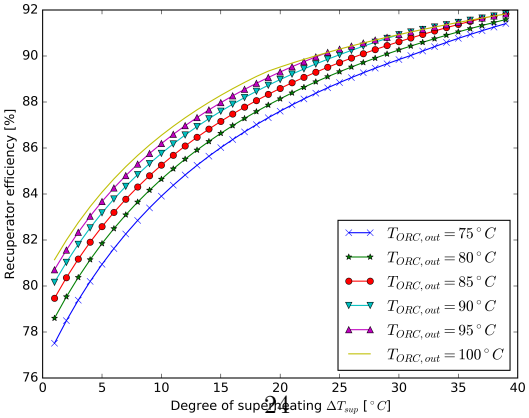

(c) Recuperator efficiency

Figure 8: Influence of the degree of superheating on the plant performance, for multiple values of $T_{b,ORCout}$.

which corresponds to the *kink* on, the turbine inlet temperature is the same ($= 125°C$), hence for the constant turbine efficiency also the turbine outlet temperature is the same. As a result also the recuperator efficiency is the same for different values of $T_{b,ORCout}$.

5. Summary and conclusions

In this paper, we have compared the performance of the series and parallel configuration of a low-temperature geothermally-fed CHP plant, coupled to thermal networks. The performance of the series and the parallel configuration has been shown as a function of the supply and return temperature of the DH system. Three constant values for the heat demand have been considered: a low heat demand of $\dot{Q}_{DH} = 3MW$, a medium heat demand of $\dot{Q}_{DH} = 6MW$ and a high heat demand of $\dot{Q}_{DH} = 9MW$. As a case study, two types of thermal networks have been investigated. On the one hand, a third generation thermal network which is today's state-of-the-art, and on the other hand, a fourth generation thermal network which operates at lower temperatures and is most likely to be introduced in future integrated and sustainable energy systems [19]. The geothermal source has a temperature of $130°C$ and is available at a flow rate of 194 kg/s.

Whether the parallel or the series configuration is the most appropriate depends on the temperature levels of the DH system. In general, the parallel configuration has the best performance for high DH temperatures, whereas the series configuration performs better for low DH temperatures. For the considered third generation 80/60 thermal network, the parallel configuration is the most appropriate. For a heat demand of $\dot{Q}_{DH} = 6MW$, the net electric power production and exergetic plant efficiency are $\dot{W}_{net} = 5.48MW$ and $\eta_{ex} = 41.25\%$, respectively. However, for the considered fourth generation 50/30 thermal network, the series configuration is more appropriate. For a heat demand of $\dot{Q}_{DH} = 6MW$, the net electric power production and exergetic plant efficiency are $\dot{W}_{net} = 6.18MW$ and $\eta_{ex} = 42.63\%$, respectively. For the considered 50/30 thermal network, the electric power production is as high as for a pure electrical power plant, but the overall plant efficiency is higher due to the utilization of the "ORC waste heat". For both cases considered, the exergetic plant efficiency of the CHP plant is higher than the one for a pure electrical power plant. So we can conclude that the combined heat-and-power production might improve the overall plant economics.

Also, the usefulness of a recuperator has been discussed. The implementation of a recuperated ORC is only useful when the ORC outlet temperature is constrained. For the parallel configuration, the ORC outlet temperature does not depend on the DH system requirements. The parallel configuration with a recuperated ORC has the same performance as the basic ORC. However, for the series configuration, the ORC outlet temperature is constrained by the supply temperature of the DH system. Therefore, the implementation of a recuperator might be useful. For R236ea, the recuperated ORC has a better performance for $T_{supply} \geq 57.15°C$ for a fixed pinch-point-temperature difference of $5°C$.

In contrast to what is often found in the literature, superheating might improve the ORC electrical power output for isentropic and dry working fluids. We have discussed the degree of superheating for the slightly dry working fluid R236ea. For the basic ORC, the ORC outlet temperature should be constrained to a temperature higher than $109°C$ to get performance improvements. But for the recuperated ORC, we have found that for all ORC outlet temperatures higher than $80°C$, the electrical power output can be increased by using superheating.

For future work, we plan to implement part-load and thermo-economic models for the CHP systems. Based on these thermo-economic (optimization) model results, we will be able to compare the economics of the different CHP configurations.

Acknowledgments

This project receives the support of the European Union, the European Regional Development Fund ERDF, Flanders Innovation & Entrepreneurship and the Province of Limburg.

Nomenclature

Abbreviations

abbr.	description
CHP	Combined Heat and Power
DH	District Heating
EOS	Equation Of State
ORC	Organic Rankine Cycle

Symbols

symbol	description
$\dot{E}x$ [MW]	flow exergy
ex [kJ/kg]	specific flow exergy
h [kJ/kg]	specific enthalpy
$\dot{I}$ [MW]	irreversibility
$\dot{m}$ [kg/s]	mass flow rate
p [bar]	pressure
$\dot{Q}$ [MW]	heat
s [kJ/kgK]	specific entropy
T [$^\circ C$]	temperature
$\dot{W}$ [MW]	power
w [kJ/kg]	specific work
η [%]	efficiency

Subscripts

symbol	description
1	wf state at pump inlet
2	wf state at pump outlet
3	wf state at turbine inlet
4	wf state at turbine outlet
b	brine
c	cooling water
$cond$	condenser
en	energetic
$evap$	evaporator
ex	exergetic
g	generator
in	inlet
m	motor
net	net
out	outlet
p	pump
$pinch$	pinch point
$recup$	recuperator
ref	reference state
$return$	return state DH system
s	isentropic
sup	superheating
$supply$	supply state DH system
t	turbine
wf	working fluid

References

[1] IEA, Technology Roadmap - Geothermal Heat and Power, Technical Report, OECD, Paris, 2011. URL: https://www.iea.org/newsroomandevents/pressreleases/2011/june/how-to-achieve-at-least-a-tenfold-increase-in-supply-of-geothermal-power-and-hea.html.

[2] MIT, The Future of Geothermal Energy: Impact of Enhanced Geothermal Systems (EGS) on the United States in the 21st Century, November, Cambridge, UK, 2006. URL: http://www.eere.energy.gov/geothermal/pdfs/structure_outcome.pdf.

[3] R. DiPippo, Geothermal Power Plants: Principles , Applications , Case Studies and Environmental Impact, third ed., 2005.

[4] F. Heberle, D. Brüggemann, Exergy based fluid selection for a geothermal Organic Rankine Cycle for combined heat and power generation, Applied Thermal Engineering 30 (2010) 1326–1332.

[5] D. Walraven, B. Laenen, W. D'haeseleer, Comparison of thermodynamic cycles for power production from low-temperature geothermal heat sources, Energy Conversion and Management 66 (2013) 220–233.

[6] A. Franco, Power production from a moderate temperature geothermal resource with regenerative Organic Rankine Cycles, Energy for Sustainable Development 15 (2011) 411–419.

[7] M. Li, J. Wang, W. He, L. Gao, B. Wang, S. Ma, Y. Dai, Construction and preliminary test of a low-temperature regenerative Organic Rankine Cycle (ORC) using R123, Renewable Energy 57 (2013) 216–222.

[8] Y. Dai, J. Wang, L. Gao, Parametric optimization and comparative study of organic Rankine cycle (ORC) for low grade waste heat recovery, Energy Conversion and Management 50 (2009) 576–582.

[9] J. Li, G. Pei, Y. Li, D. Wang, J. Ji, Energetic and exergetic investigation of an organic Rankine cycle at different heat source temperatures, Energy 38 (2012) 85–95.

[10] B. F. Tchanche, G. Lambrinos, A. Frangoudakis, G. Papadakis, Low-grade heat conversion into power using organic Rankine cycles A review of various applications, Renewable and Sustainable Energy Reviews 15 (2011) 3963–3979.

[11] S. Quoilin, M. V. D. Broek, S. Declaye, P. Dewallef, V. Lemort, Techno-economic survey of Organic Rankine Cycle (ORC) systems, Renewable and Sustainable Energy Reviews 22 (2013) 168–186.

[12] B. Saleh, G. Koglbauer, M. Wendland, J. Fischer, Working fluids for low-temperature organic Rankine cycles, Energy 32 (2007) 1210–1221.

[13] H. Chen, D. Y. Goswami, E. K. Stefanakos, A review of thermodynamic cycles and working fluids for the conversion of low-grade heat, Renewable and Sustainable Energy Reviews 14 (2010) 3059–3067.

[14] A. Müller, J. Winkelmann, J. Fischer, Backone family of equations of state: 1. Nonpolar and polar pure fluids, AIChE Journal 42 (1996) 1116–1126.

[15] C. Rubio-Maya, V. M. Ambríz Díaz, E. Pastor Martínez, J. M. Belman-Flores, Cascade utilization of low and medium enthalpy geothermal resources - A review, Renewable and Sustainable Energy Reviews 52 (2015) 689–716.

[16] T. Li, J. Zhu, W. Zhang, Comparative analysis of series and parallel geothermal systems combined power, heat and oil recovery in oilfield, Applied Thermal Engineering 50 (2013) 1132–1141.

[17] M. Habka, S. Ajib, Determination and evaluation of the operation characteristics for two configurations of combined heat and power systems depending on the heating plant parameters in low-temperature geothermal applications, Energy Conversion and Management 76 (2013) 996–1008.

[18] M. Habka, S. Ajib, Investigation of novel, hybrid, geothermal-energized cogeneration plants based on organic Rankine cycle, Energy 70 (2014) 212–222.

[19] H. Lund, S. Werner, R. Wiltshire, S. Svendsen, J. E. Thorsen, F. Hvelplund, B. V. Mathiesen, 4th Generation District Heating (4GDH), Energy 68 (2014) 1–11.

[20] VITO, Diepe geothermie in de Kempen: what's next?, 2017. URL: https://vito.be/nl/media-events/nieuws/diepe-geothermie-de-kempen-whats-next.

[21] Y.-R. Li, J.-N. Wang, M.-T. Du, S.-Y. Wu, C. Liu, J.-L. Xu, Effect of pinch point temperature difference on cost-effective performance of organic Rankine cycle, International Journal of Energy Research 31 (2013).

[22] J. Calm, G. Hourahan, Physical, safety and environmental data for current and alternative refrigerants, in: International Congress of Refrigeration, Prague, Czech Republic, 2011. URL: http://www.hourahan.com/wp/wp-content/uploads/2010/08/2011-Physical-Safety-and-Environmental-Data2.pdf.

[23] G. van Rossum, Python Tutorial, Technical Report CS-R9526, Technical Report, Centrum voor Wiskunde en Informatica (CWI), Amsterdam, 1995. URL: http://www.python.org.

[24] J. Andersson, A General-Purpose Software Framework for Dynamic Optimization, Phd, Arenberg Doctoral School, KU Leuven, 2013.

[25] A. Wächter, L. T. Biegler, On the implementation of an interior-point filter line-search algorithm for large-scale nonlinear programming, Mathematical Programming 106 (2006) 25–57.

[26] E. Lemmon, M. Huber, M. McLinden, REFPROP - Reference Fluid Thermodynamic and Transport Properties. NIST Standard Reference Database 23, 2007.

[27] H. Gadd, S. Werner, Achieving low return temperatures from district heating substations, Applied Energy 136 (2014) 59–67.

[28] EUDP, Full-scale demonstration of low temperature district heating in existing buildings, 2010. URL: https://setis.ec.europa.eu/energy-research/sites/default/files/project/docs/GuidelinesforLTDH-final_rev1.pdf.